Hindawi Publishing Corporation
Mathematical Problems in Engineering
Volume 2009, Article ID 965603, 13 pages
doi:10.1155/2009/965603

Research Article

Thermal Radiation Effects on Heat and Mass Transfer over an Unsteady Stretching Surface

Stanford Shateyi[1] and Sandile Sydney Motsa[2]

[1] *Department of Mathematics, University of Venda, Private Bag X5050, Thohoyandou 0950, South Africa*
[2] *Department of Mathematics, University of Swaziland, Private Bag 4, Kwaluseni M201, Swaziland*

Correspondence should be addressed to Stanford Shateyi, stanford.shateyi@univen.ac.za

Received 9 June 2009; Revised 25 September 2009; Accepted 5 November 2009

Recommended by Mehrdad Massoudi

The unsteady heat, mass, and fluid transfer over a horizontal stretching sheet has been numerically investigated. Using a similarity transformation the governing time-dependent boundary layer equations for the momentum, heat, and mass transfer were reduced to a sets of ordinary differential equations. These set of ordinary differential equations were then solved using the Chebyshev pseudo-spectral collocation method, and a parametric analysis was carried out. The study observed, among other observations that the local Sherwood number increases as the values of the stretching parameter A and the Schmidt number Sc increase. Also the fluid temperature was found to be significantly reduced by increases in the values of the Prandtl number Pr, the unsteadiness parameter A, and the radiation parameter R. The velocity and concentration profiles were found to be reduced by increasing values of the unsteadiness parameter A.

1. Introduction

The continuous surface heat and mass transfer problem has many practical applications in industrial manufacturing processes. The knowledge of flow and heat and mass transfer within a thin liquid film is crucial in understanding the coating process and design of heat exchangers and chemical processing equipments. This phenomenon is also applied in wire and fibre coatings, food stuff processing reactor fluidization, and transpiration cooling. The prime aim in almost every extrusion is to maintain the surface quality of the extrudate. The problem of extrusion of thin surface layers needs special attention to gain some knowledge for controlling the coating efficiently. In the pioneering work of Crane [1], the flow of Newtonian fluid over a linearly stretching surface was studied. Subsequently, the pioneering works of Crane are extended by many authors to explore various aspects of the flow and heat transfer occurring in an infinite domain of the fluid surrounding the stretching sheet (see [2–8]). However, these studies dealt with a steady flow only. In some cases the flow field and

heat transfer can be unsteady due to a sudden stretching of the flat sheet or by a steep change of the temperature of the sheet.

Hossain et al. [9] determined the effect of radiation on natural convection flow of an optically thick viscous incompressible flow past a heated vertical porous plate with a uniform surface temperature and a uniform rate of suction where radiation is included by assuming the Rosseland discussion approximation.

Andersson et al. [10] investigated using a similarity transformation the flow of a thin liquid film of a power-law fluid by unsteady stretching of a surface. Later on, Andersson et al. [11] analyzed the momentum and heat transfer in a laminar liquid film on a horizontal stretching sheet governed by time-dependent boundary layer equations. Dandapat et al. [12] explored how the hydrodynamics and heat transfer in a liquid film on unsteady stretching surface are affected by thermo-capillarity. Tsai et al. [13] studied the non-uniform heat source/sink effect on the flow and heat transfer from an unsteady stretching sheet through a quiescent fluid medium extending to infinity.

Liu and Andersson [14] generalized the analysis by Andersson et al. [11] of the thermal characteristics of a liquid film driven by an unsteady stretching surface. Here, they considered a more general form of the prescribed temperature variation of the stretching sheet than that considered in Andersson et al. [11].

Elbashbeshy and Bazid [15] presented similarity solutions of the boundary layer equations, which describe the unsteady flow and heat transfer over an unsteady stretching sheet. However, as was to be later discovered by Abd El-Aziz [16], some physically unrealistic phenomena are encountered for specific values of the unsteadiness parameter. To that end, Abd El-Aziz [16] was concerned with correcting the similarity transformation introduced by Elbashbeshy and Bazid [15] and extended their analysis to include the effect of thermal radiation. Thermal radiation plays a very significant role in controlling heat transfer in polymer processing industry. The quality of the final product depends to a great extend on the heat controlling factors, and the knowledge of radiative heat transfer in the system can perhaps lead to a desired product with sought qualities.

In this paper, we extend the work of Abd El-Aziz [16] to include mass transfer. This problem arises in a number of industrial manufacturing processes such as polymer extrusion, wire drawing, metal and plastic extrusion, continuous casting, glass fibre production, crystal growing and paper production. The physical and thermal characteristics of such unsteady process are investigated in the boundary layer approximation, assuming variation of the surface temperature and concentration with the horizontal coordinate x and time, t. The main objective of this work is to try to solve this type of model using Chebyshev pseudospectral collocation method. In previous studies finite-difference, Runge-Kutta integration schemes were used. However, it is now known that Chebyshev pseudospectral collocation method gives better approximations than most of these numerical methods. Our main focus is on the comparison of the results obtained by Chebyshev pseudospectral collocation method and those obtained by Abd El-Aziz [16]. We also look at the effects of the unsteadiness parameter on the concentration characteristics of the overlying above the stretching surface.

2. Problem Formulation

We consider the flow of a viscous and incompressible fluid on a horizontal sheet, which comes through a slot at the origin. We are considering a gray, absorbing-emitting radiation fluid but nonscattering medium, and the Rosseland approximation is used to describe the radiative

heat flux in the energy equation. The radiative heat flux in the x-direction is negligible in comparison with that in the y-direction. The fluid flow over the unsteady stretching sheet is composed of a reacting chemical species. The fluid motion arises due to the stretching of the elastic sheet. The continuous sheet aligned with the x-axis at $y = 0$ moves in its own plane with a velocity $U_w(x,t)$, the temperature distribution $T_w(x,t)$ and the concentration distribution $C_w(x,t)$ vary both along the sheet and with time. The velocity, temperature, and concentration fields in the boundary layer are governed by the two-dimensional boundary layer equations for mass, momentum, thermal energy, and chemical species given by:

$$\frac{\partial u}{\partial x} + \frac{\partial v}{\partial y} = 0, \tag{2.1}$$

$$\frac{\partial u}{\partial t} + u\frac{\partial u}{\partial x} + v\frac{\partial u}{\partial y} = \nu\frac{\partial^2 u}{\partial y^2}, \tag{2.2}$$

$$\frac{\partial T}{\partial t} + u\frac{\partial T}{\partial x} + v\frac{\partial T}{\partial y} = \alpha_0\frac{\partial^2 T}{\partial y^2} - \frac{1}{\rho c_p}\frac{\partial q_r}{\partial y}, \tag{2.3}$$

$$\frac{\partial C}{\partial t} + u\frac{\partial C}{\partial x} + v\frac{\partial C}{\partial y} = D\frac{\partial^2 C}{\partial y^2}, \tag{2.4}$$

where u and v are the velocity components along the x- and y-axes, respectively, T is the fluid, temperature, C is the concentration, ν is the kinematic coefficient of viscosity, $\alpha_0 = k/\rho c_p$ is the thermal diffusivity with k as the fluid thermal conductivity, ρ the fluid density, c_p the specific heat at constant pressure, D the mass diffusivity, and q_r as the radiative heat flux.

By using the Rosseland diffusion approximation (Hossain et al. [9]) and following Raptis [17] among other researchers, the radiative heat flux, q_r is given by

$$q_r = -\frac{4\sigma^*}{3k_1}\frac{\partial T^4}{\partial y}, \tag{2.5}$$

where σ^* and k_1 are the Stefan-Boltzman constant and the Roseland mean absorption coefficient, respectively. We assume that the temperature differences within the flow are sufficiently small such that T^4 may be expressed as a linear function of temperature

$$T^4 \approx 4T_\infty^3 T - 3T_\infty^4. \tag{2.6}$$

Using (2.5) and (2.6) in the last term of (2.3), we obtain

$$\frac{\partial q_r}{\partial y} = -\frac{16\sigma^* T_\infty^3}{3k_1\rho c_p}\frac{\partial^2 T}{\partial y^2}. \tag{2.7}$$

The associated boundary conditions for the model are

$$u(x,0) = U_w(x,t), \qquad v(x,0) = 0, \qquad T(x,0) = T_w(x,t), \qquad C(x,0) = C_w(x,t), \tag{2.8}$$

$$u(x,\infty) = 0, \qquad T(x,\infty) = T_\infty, \qquad C(x,\infty) = C_\infty. \tag{2.9}$$

Following Andersson et al. [10], the stretching velocity $U_w(x,t)$ is assumed $U_w = bx/(1-\alpha t)$, where both b and α are positive constants with dimension reciprocal time. We have b as the initial stretching rate $b/(1-\alpha t)$ is increasing with time. In the context of polymer extrusion, the material properties and in particular the elasticity of the extruded sheet may vary with time even though the sheet is being pulled by a constant force.

With unsteady stretching, however, α^{-1} becomes the representative time scale of the resulting unsteady boundary layer problem. We assume both the surface temperature $T_w(x,t)$ and the surface concentration $C_w(x,t)$ of the stretching sheet to vary with the distance x along the sheet and time in the following form:

$$T_w(x,t) = T_\infty + T_0\left[\frac{bx^2}{\nu}\right](1-\alpha t)^{-3/2}, \tag{2.10}$$

$$C_w(x,t) = C_\infty + C_0\left[\frac{bx^2}{\nu}\right](1-\alpha t)^{-3/2}, \tag{2.11}$$

where T_0 is a heating or cooling reference temperature and C_0 is a positive concentration reference. The equation for the temperature increases (reduces) if T_0 is positive (negative) from T_0 at the leading edge in proportion to x^2 and such that the amount of temperature increase (reduction) along the sheet increases with time. The equation for the concentration $C(x,t)$ of the sheet also represents a situation in which the sheet species increases if C_0 is positive from C_0 at the leading edge in proportion to x^2 and such that the amount of concentration increase along the sheet increases with time. In order to reduce (2.1)–(2.4) into a set of convenient ordinary differential equations, we introduce the similarity variable η and the dimensionless variables f, θ, and ϕ (Abd El-Aziz [16]) as:

$$\begin{aligned} &\psi = (\nu b)^{1/2}(1-\alpha t)^{-1/2} x f(\eta), \qquad \eta = \left(\frac{b}{\nu}\right)^{1/2}(1-\alpha t)^{-1/2} y, \\ &T = T_\infty + T_0\left[\frac{bx^2}{2\nu}\right](1-\alpha t)^{-3/2}\theta(\eta), \qquad C = C_\infty + C_0\left[\frac{bx^2}{2\nu}\right](1-\alpha t)^{-3/2}\phi(\eta), \end{aligned} \tag{2.12}$$

where $\psi(x,y)$ is the physical stream function which automatically satisfies the continuity equation. The velocity components are then derived from the stream function expression and obtained as

$$u = \frac{\partial \psi}{\partial y} = U_w f'(\eta), \qquad v = -\frac{\partial \psi}{\partial x} = -(\nu b)^{1/2}(1-\alpha t)^{-1/2} f(\eta). \tag{2.13}$$

Governing equations are then transformed into a set of differential equations and associated boundary conditions as given below:

$$f''' + ff'' - (f')^2 - A\left(f' + \frac{\eta}{2}f''\right) = 0, \tag{2.14}$$

$$(3R+4)\theta'' + 3R\mathrm{Pr}\left[f\theta' - 2f'\theta - \frac{A}{2}(3\theta + \eta\theta')\right] = 0, \tag{2.15}$$

$$\phi'' + \mathrm{Sc}\left[f\phi' - 2f'\,\phi - \frac{A}{2}(3\phi + \eta\phi')\right] = 0, \tag{2.16}$$

where the prime indicates differentiation with respect to η, $A = \alpha/b$ is the unsteady parameter, $\theta = (T - T_\infty)/(T_w - T_\infty)$ is the non-dimensional temperature, $\phi = (C - C_\infty)/(C_w - C_\infty)$ is the non-dimensional concentration, $R = kk_1/3\sigma^* T_\infty^3$ is the radiation parameter, $\mathrm{Pr} = \nu/\alpha_0$ is the Prandtl number and $\mathrm{Sc} = \nu/D$ is the Schmidt number. We note that equations (2.15) and (2.16) are equivalent if Sc in equation (2.16) is replaced by $3R\mathrm{Pr}/(3R+4)$. In view of equations (2.12), the boundary conditions from (2.8) to (2.10), transform into

$$f(0) = 0, \qquad f'(0) = 1, \qquad \theta(0) = \phi(0) = 1, \tag{2.17}$$

$$f'(\infty) = 0, \qquad \theta(\infty) = 0, \qquad \phi(\infty) = 0. \tag{2.18}$$

3. Method of Solution

To solve the governing equations (2.14)–(2.17), we use the Chebyshev pseudospectral collocation method. The domain in the η direction is approximated by $[0, L]$, where L is the edge of the boundary layer. We use the algebraic mapping $\eta = (Y+1)L/2$ to map the physical region into the Chebyshev spectral method computation domain of $[-1, 1]$. The unknown variables f, θ, and ϕ in (2.14)–(2.17) are approximated by the following truncated series of polynomials:

$$f(Y) = \sum_{k=0}^{N} \hat{f}_k T_k(Y), \qquad \theta(Y) = \sum_{k=0}^{N} \hat{\theta}_k T_k(Y), \qquad \phi(Y) = \sum_{k=0}^{N} \hat{\phi}_k T_k(Y), \tag{3.1}$$

where the values $\hat{f}_k$, $\hat{\theta}_k$, and $\hat{\phi}_k$ are the coefficients of the series to be determined, T_k is the Chebyshev polynomial of degree k which is defined on the interval $Y \in [-1, 1]$ as

$$T_k(Y) = \cos\left(k\cos^{-1}Y\right), \quad k = 0, 1, \ldots. \tag{3.2}$$

We use the Gauss-Lobatto collocation points to define the Chebyshev nodes in $[-1, 1]$, namely;

$$Y_j = \cos\frac{\pi j}{N} \quad -1 \le Y \le 1, \; j = 0, 1, \ldots, N. \tag{3.3}$$

Derivatives of the functions f, θ, and ϕ at the collocation points are represented as

$$\frac{df}{d\eta} = \frac{2}{L}\sum_{k=0}^{N}\mathbf{D}_{jk}\widehat{f}_k, \qquad \frac{d\theta}{d\eta} = \frac{2}{L}\sum_{k=0}^{N}\mathbf{D}_{jk}\widehat{\theta}_k, \qquad \frac{d\phi}{d\eta} = \frac{2}{L}\sum_{k=0}^{N}\mathbf{D}_{jk}\widehat{\phi}_k, \tag{3.4}$$

where $\mathbf{D}$ is the Chebyshev spectral method differentiation matrix (see, e.g., Canuto et. al [18] for details). Higher order derivatives are computed as multiple powers of $\mathbf{D}$, that is, (with f as an example)

$$\frac{d^i f}{d\eta^i} = \left(\frac{2}{L}\right)^i \sum_{k=0}^{N}\mathbf{D}_{jk}^i\widehat{f}_k, \quad k = 0, 1, 2\ldots, N, \tag{3.5}$$

where i is the order of the derivative.

Substituting (3.1)–(3.5) into the governing equations and boundary conditions (2.14)–(2.17), we obtain the following equations:

$$\overline{\mathbf{D}}^3\mathbf{F} + \mathbf{F}\overline{\mathbf{D}}^2\mathbf{F} - \left(\overline{\mathbf{D}}\mathbf{F}\right)\left(\overline{\mathbf{D}}\mathbf{F}\right) - A\left(\overline{\mathbf{D}}\mathbf{F} + \frac{\eta}{2}\overline{\mathbf{D}}^2\mathbf{F}\right) = 0, \tag{3.6}$$

$$(3R+4)\overline{\mathbf{D}}^2\Theta + 3R\mathrm{Pr}\left[\mathbf{F}\overline{\mathbf{D}}\Theta - 2\Theta\overline{\mathbf{D}}\mathbf{F} - \frac{A}{2}\left(3\Theta + \eta\overline{\mathbf{D}}\Theta\right)\right] = 0, \tag{3.7}$$

$$\overline{\mathbf{D}}^2\Phi + \mathrm{Sc}\left[\mathbf{F}\overline{\mathbf{D}}\Phi - 2\Phi\overline{\mathbf{D}}\mathbf{F} - \frac{A}{2}\left(3\Phi + \eta\overline{\mathbf{D}}\Phi\right)\right] = 0, \tag{3.8}$$

where $\overline{\mathbf{D}} = (2/L)\mathbf{D}$, $\mathbf{F} = \{\widehat{f}_0, \widehat{f}_1, \ldots, \widehat{f}_N\}^T$, $\Theta = \{\widehat{\theta}_0, \widehat{\theta}_1, \ldots, \widehat{\theta}_N\}^T$, $\Phi = \{\widehat{\phi}_0, \widehat{\phi}_1, \ldots, \widehat{\phi}_N\}^T$ and the superscript T denotes Transpose. The boundary conditions become

$$\widehat{f}_N = 0, \quad \sum_{k=0}^{N}\widehat{\mathbf{D}}_{Nk}\widehat{f}_k = 1, \quad \sum_{k=0}^{N}\widehat{\mathbf{D}}_{0k}\widehat{f}_k = 0, \tag{3.9}$$

$$\widehat{\theta}_N = \widehat{\phi}_N = 1, \qquad \widehat{\theta}_0 = \widehat{\phi}_0 = 0. \tag{3.10}$$

We note that (3.6) can be solved separately because it depends on $\mathbf{F}$ only. To solve the system of equations we start by solving (3.6) subject to the boundary conditions (3.9) is a MATLAB nonlinear equation solver *fzero* which is based on the quasi-Newton method. Once the solution for $\mathbf{F}$ is obtained, it is then substituted into equation (3.7) to get:

$$\mathbf{B}\Theta = \mathbf{K}, \quad \text{then } \Theta = \mathbf{B}^{-1}\mathbf{K}, \tag{3.11}$$

where

$$\mathbf{B} = (3R+4)\overline{\mathbf{D}}^2 + 3R\mathrm{Pr}\left[\mathbf{F}\overline{\mathbf{D}} - 2\overline{\mathbf{D}}\mathbf{F} - \frac{A}{2}\left(3\mathbf{I} + \eta\overline{\mathbf{D}}\right)\right], \qquad \mathbf{K} = [0 \;\; 0 \;\; \cdots \;\; 0 \;\; 1]^T, \tag{3.12}$$

Table 1: Comparison of the values of $-f''(0)$, $-\theta'(0)$ and the maximum error between the exact solution and the Chebyshev spectral method.

Method	$-f''(0)$	$-\theta'(0)$	$\varepsilon^{f}_{N,L}$	$\varepsilon^{\theta}_{N,L}$
Exact	1.0000000000	2.0000000000		
Numerical	1.0000000003	1.9999999998	$2.0613826646 \times 10^{-9}$	$1.1308017023 \times 10^{-10}$

Table 2: Comparison of the Chebyshev solution for $-\theta'(0)$ with the results of El-Aziz [16].

A	Pr	El-Aziz (2009)	Present Results
0.8	0.1	0.4517	0.45149
0.8	1.0	1.6728	1.67285
0.8	10	5.70503	5.70598
1.2	0.1	0.5087	0.50850
1.2	1.0	1.818	1.81801
1.2	10	6.12067	6.12102
2	0.1	0.606013	0.60352
2	1.0	2.07841	2.07841
2	10	6.88506	6.88615

and $\mathbf{I}$ is an identity matrix of size $N+1$. The boundary conditions are imposed by setting the first and last row of $\mathbf{B}$ to be $[1 \;\; 0 \;\; \cdots \;\; 0 \;\; 0]$ and $[0 \;\; 0 \;\; \cdots \;\; 0 \;\; 1]$, respectively. The solution for (3.8) is obtained in a similar manner.

4. Results and Discussion

The nonlinear ordinary equations (2.14)–(2.16) (in the case when $A = 0$, Sc = 2, and Pr set to be $\mathrm{Pr} = 2(3R+4)/3R$) together with the associated boundary conditions have exact solutions in the form

$$f(\eta) = 1 - e^{-\eta}, \qquad \theta(\eta) = e^{-2\eta}, \qquad \phi(\eta) = e^{-2\eta}. \tag{4.1}$$

To validate out numerical method of solution, we compared our numerical results to exact solution (4.1). Table 1 presents the comparison between the exact solution and the Chebyshev spectral method of the skin friction $-f''(0)$ and the Nusselt number $-\theta'(0)$. The table also gives the maximum errors ($\varepsilon^{f}_{N,L}$ and ($\varepsilon^{\theta}_{N,L}$)) which refer to the maximum difference between the approximated and exact values of f and θ at the Gauss-Lobatto collocation points. In computing the numerical results, we used $L = 20$ and $N = 100$.

From Table 1 it can be seen that the Chebyshev spectral method is in good agreement with the exact solution for the skin friction, Nusselt number, and the values of f and θ. Figure 1 shows the numerical solutions for the velocity and temperature profiles compared against the exact solutions (4.1). As depicted in this figure, Chebyshev spectral method gives excellent approximations to the model under consideration.

The present numerical results were also compared with results of El-Aziz [16] (see Table 2).

In Table 2, we have the data comparisons with the previous published paper and the results are found to be in excellent agreement. It is clearly seen in this table that for given

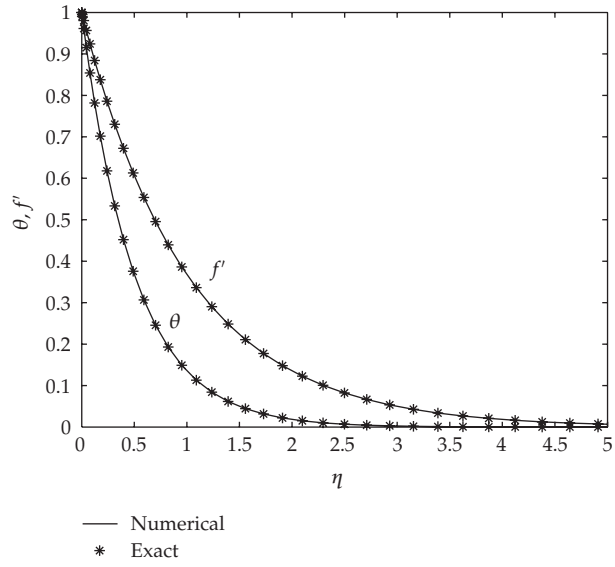

Figure 1: Graph of the velocity f' and temperature θ profiles plotted against the exact solutions with $A = 1$, $R = 1$, Pr = 0.7, Sc = 0.2.

values of A, the local Nusselt number is increased as the Prandtl number increases. Also, when all other parameters are kept constant, higher local Nusselt number are observed at larger values of Pr. This can be elucidated from the fact that as the Prandtl number increases, the thermal boundary layer thickness decreases and the wall gradient increases. We can also observe in this table that for fixed values of Pr, the local Nusselt number increases as the unsteadiness parameter A increases.

Figure 2 illustrates the concentration profile for Sc = 0.2 and varying unsteadiness parameters $A = 0$, 0.5, and 2.0. The results show that the concentration $\phi(\eta)$ decreases with increases in the values of the unsteadiness parameter.

In Figure 3, we have the local Sherwood number in terms of $-\phi'(0)$ as a function of the unsteadiness parameter A for some typical Schmidt number values. It can be clearly seen from this figure that the Sherwood number is increased as the values of the Schmidt number increase. We can also see that, for a given value of A, higher Sherwood number values are observed at large values of Sc. This can be explained from the fact that as the Schmidt increases, the concentration boundary layer thickness decreases and the wall concentration gradient increases.

In Figure 4, we show the effect of the Schmidt number on the concentration distributions. The Schmidt number represents the relative ease of molecular momentum and mass transfer and is very important in calculations of binary mass transfer in multiphase flows. The effect of an increase in the Schmidt number values is to reduce the momentum boundary layer and this leads to the thinning of the diffusion layer. Diffusing chemical species of most interest in air have Schmidt numbers in the range from 0.1 to 10 (Hussain and Hossain [19]).

In Figure 5, we elucidate the effect of the unsteadiness parameter A on the typical temperature profiles. At fixed values of other parameters, increasing A values, decreases the temperature with an accompanying decreases in the boundary layer thickness.

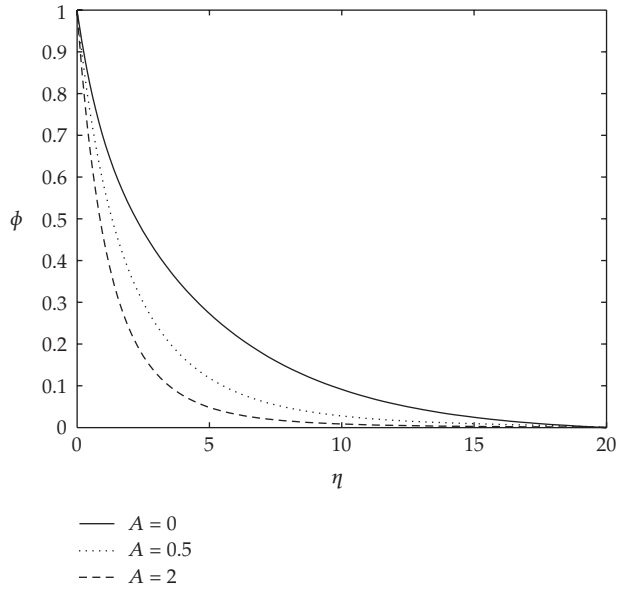

Figure 2: Effect of various values of unsteadiness parameter A on ϕ at Sc = 0.2, $R = 1$, Pr = 0.7.

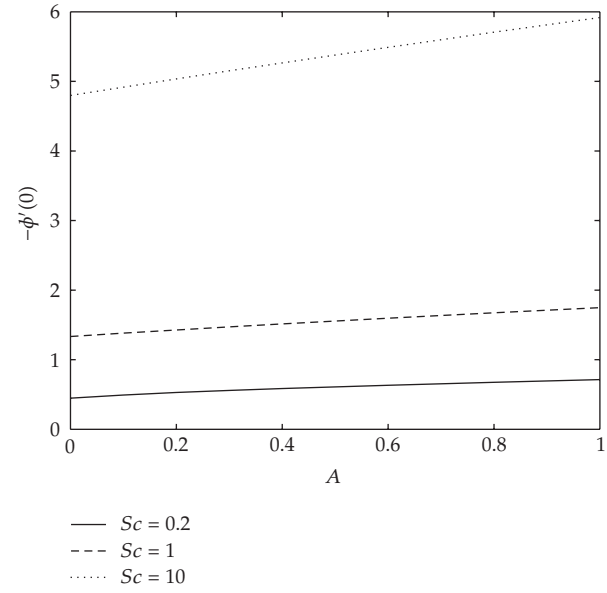

Figure 3: Local Sherwood number $-\phi'(0)$ versus A for various values of Sc with $R = 1$, Pr = 0.7.

The effects of the Prandtl number on the temperature distributions in the boundary layer are illustrated in Figure 6. We observe that the thermal boundary layer is reduced by increasing the Prandtl number values thereby reducing the fluid temperature. The effects of thermal radiation parameter R on the temperature profiles in the boundary layer are illustrated in Figure 7. We observe in this figure that increasing the thermal radiation parameter produces significant decrease in the thermal condition of fluid and its boundary

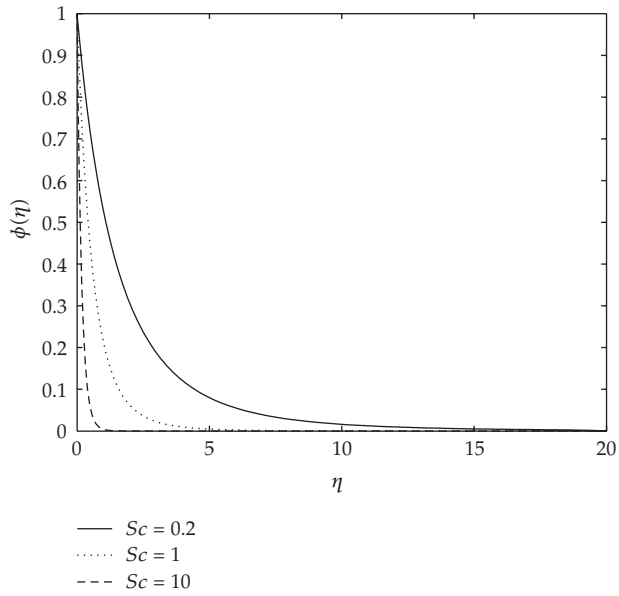

Figure 4: Effect of varying the Schmidt number Sc on the concentration profiles with Pr = 0.7, $A = 1$, $R = 1$.

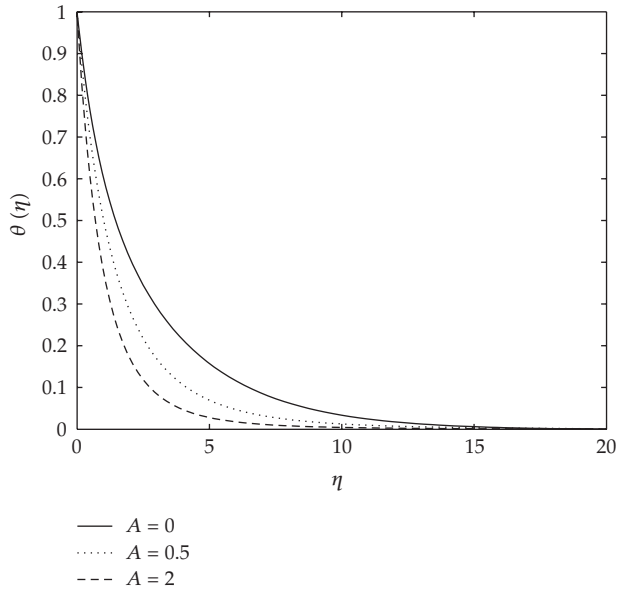

Figure 5: Effect of various values of unsteadiness parameter A on on the temperature profiles with Pr = 0.7, Sc = 0.2, $R = 1$.

layer. This can be explained by the fact that a decrease in the values of $R(= kk_1/3\sigma T_\infty^3)$ for the given values of k and T_∞ means a decrease in the Rosseland radiation absorptivity k_1. We can deduce in equations (2.3) and (2.5) that the divergence of the radiative heat flux $\partial q_r/\partial y$ increases as k_1 decreases the rate of radiative heat transferred to the fluid and consequently the fluid temperature increases. It is shown in Figure 7 the effect of thermal radiation becomes

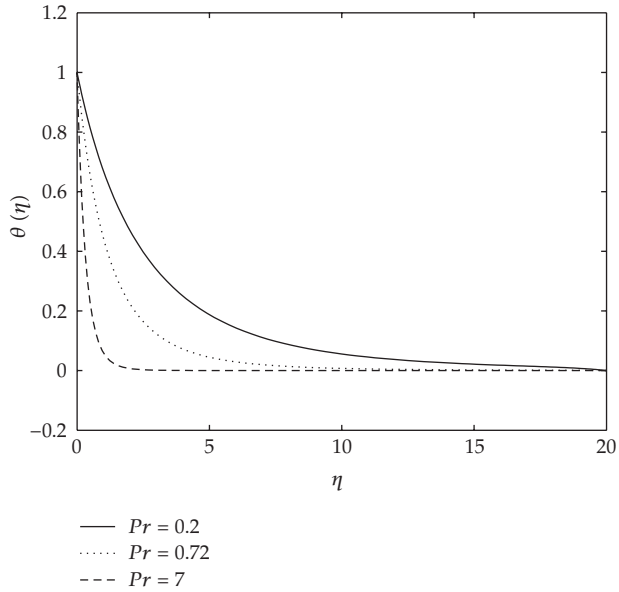

Figure 6: The variation of the temperature distribution profiles with increasing Prandtl number.

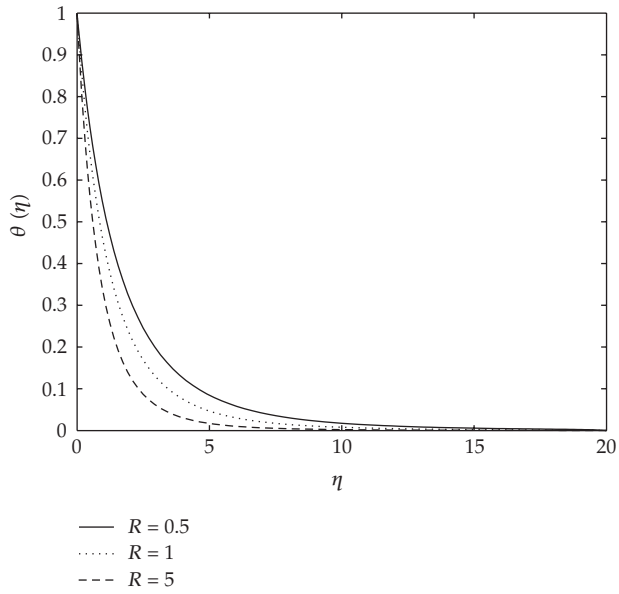

Figure 7: The variation of the temperature distribution profiles with increasing thermal radiation parameter.

more significant as $R \to 0$ though not equals to zero and $R = \infty$ corresponds to non-radiating case so the effects of radiation can be neglected when $R \to \infty$.

In Figure 8, we present velocity profiles when all other parameters are kept constant for different values of the unsteadiness parameter A. We observe in this figure that the velocity decreases with the distance from the stretching sheet for all A. Also, increasing the

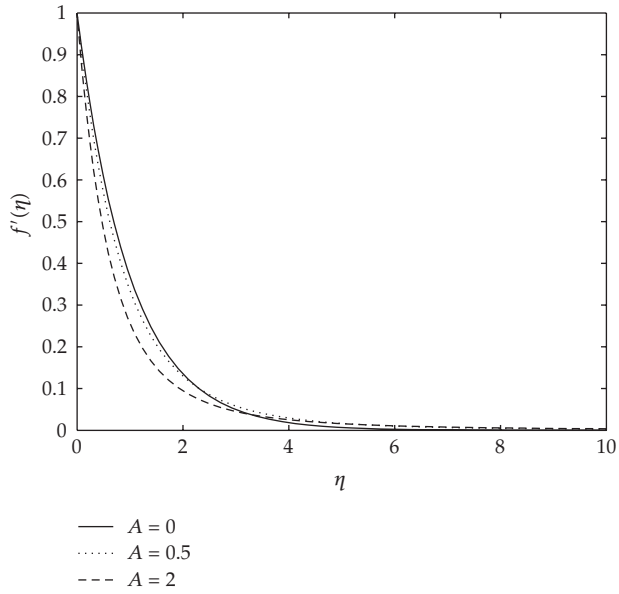

Figure 8: Effect of various values of unsteadiness parameter A on on the velocity profiles.

values of A decreases the velocity in the boundary layer. When $A = 0$, we have a steady state flow and for $A > 0$, we have an unsteady flow. As can be seen in Figures 2, 5, and 8, increasing the unsteadiness parameter A reduces the flow properties such as velocity, temperature and concentration. When A values are increased in the system, the boundary layer thicknesses are reduced and this inhibits the development of transition of laminar to turbulent flow. This shows that stretching of surfaces can be used as a flow stabilizing mechanism.

5. Conclusion

The unsteady heat, mass, and fluid transfer over a horizontal stretching sheet has been investigated in this study. The study put much emphasis on the numerical method used to solve the set of non-linear ordinary differential equations and on how the concentration distribution and mass transfer change due to stretching of the sheet. The study found out that the Nusselt number increases with the increase of the unsteadiness parameter and Prandtl number. The fluid temperature was found to be reduced by increases in the values of the unsteadiness parameter, Prandtl number and the radiation parameter. We also observed that the velocity profiles and the concentration distributions were reduced as the values of the unsteadiness parameter A were increased. The local Sherwood number was found to be increased by the increased values of A and the Schmidt number.

References

[1] L. J. Crane, "Flow past a stretching plate," *Zeitschrift für angewandte Mathematik und Physik*, vol. 12, pp. 645–647, 1970.

[2] M. K. Laha, P. S. Gupta, and A. S. Gupta, "Heat transfer characteristics of the flow of an incompressible viscous fluid over a stretching sheet," *Warme und Stoffubertrag*, vol. 24, no. 3, pp. 151–153, 1989.

[3] N. Afzal, "Heat transfer from a stretching surface," *International Journal of Heat and Mass Transfer*, vol. 36, no. 4, pp. 1128–1131, 1993.
[4] K. V. Prasad, A. S. Abel, and P. S. Datti, "Diffusion of chemically reactive species of non-Newtonian fluid immersed in a porous medium over a stretching sheet," *The International Journal of Non-Linear Mechanics*, vol. 38, no. 5, pp. 651–657, 2003.
[5] M. S. Abel and N. Mahesha, "Heat transfer in MHD viscoelastic fluid flow over a stretching sheet with variable thermal conductivity, non-uniform heat source and radiation," *Applied Mathematical Modelling*, vol. 32, no. 10, pp. 1965–1983, 2008.
[6] P. G. Abel, Siddheshwar, and M. M. Nandeppanava, "Heat transfer in a viscoelastic boundary layer flow over a stretching sheet with viscous dissipation and non-uniform heat source," *International Journal of Heat and Mass Transfer*, vol. 50, no. 5-6, pp. 960–966, 2007.
[7] R. Cortell, "Viscoelastic fluid flow and heat transfer over a stretching sheet under the effects of a non-uniform heat source, viscous dissipation and thermal radiation," *International Journal of Heat and Mass Transfer*, vol. 50, no. 15-16, pp. 3152–3162, 2007.
[8] C. Wang, "Analytic solutions for a liquid film on an unsteady stretching surface," *Heat and Mass Transfer*, vol. 42, pp. 43–48, 2006.
[9] M. A. Hossain, M. A. Alim, and D. A. S. Rees, "The effect of radiation on free convection from a porous vertical plate," *International Journal of Heat and Mass Transfer*, vol. 42, no. 1, pp. 181–191, 1999.
[10] H. I. Andersson, J. B. Aarseth, N. Braud, and B. S. Dandapat, "Flow of a power-law fluid film on an unsteady stretching surface," *Journal of Non-Newtonian Fluid Mechanics*, vol. 62, no. 1, pp. 1–8, 1996.
[11] H. I. Andersson, J. B. Aarseth, and B. S. Dandapat, "Heat transfer in a liquid film on unsteady stretching surface," *International Journal of Heat and Mass Transfer*, vol. 43, no. 1, pp. 69–74, 2000.
[12] B. S. Dandapat, B. Santra, and H. I. Andersson, "Thermocapillary in a liquid film on an unsteady stretching surface," *International Journal of Heat and Mass Transfer*, vol. 46, pp. 3009–3015, 2003.
[13] R. Tsai, K. H. Huang, and J. S. Huang, "Flow and heat transfer over an unsteady stretching surface with non-uniform heat source," *International Communications in Heat and Mass Transfer*, vol. 35, no. 10, pp. 1340–1343, 2008.
[14] I.-C. Liu and H. I. Andersson, "Heat transfer in a liquid film on an unsteady stretching sheet," *International Journal of Thermal Sciences*, vol. 47, no. 6, pp. 766–772, 2008.
[15] E. M. A. Elbashbeshy and M. A. A. Bazid, "Heat transfer over an unsteady stretching surface with internal heat generation," *Applied Mathematics and Computation*, vol. 138, no. 2-3, pp. 239–245, 2003.
[16] M. Abd El-Aziz, "Radiation effect on the flow and heat transfer over an unsteady stretching sheet," *International Communications in Heat and Mass Transfer*, vol. 36, no. 5, pp. 521–524, 2009.
[17] A. Raptis, "Flow of a micropolar fluid past a continuously moving plate by the presence of radiation," *International Journal of Heat and Mass Transfer*, vol. 41, no. 18, pp. 2865–2866, 1998.
[18] C. Canuto, M. Y. Hussaini, A. Quarteroni, and T. Zang, *Spectral Method in Fluid Dynamics*, Springer, New York, NY, USA, 1998.
[19] S. Hussain and M. A. Hossain, "Natural convection flow from a vertical permeable flat plate with variable surface temperature and species concentration," *Engineering Computations*, vol. 17, no. 7, pp. 789–813, 2000.